Journal of Electroceramics, 7, 169–177, 2001
© 2002 Kluwer Academic Publishers. Manufactured in The Netherlands.

Grain Size Dependence of Electrical Conductivity in Polycrystalline Cerium Oxide

ANDREAS TSCHÖPE & RAINER BIRRINGER
Universität des Saarlandes, Technische Physik, Gebäude 43, 66041 Saarbrücken, Germany

Submitted June 25, 2001; Revised November 2, 2001; Accepted November 13, 2001

Abstract. The magnitude and activation energy of electrical conductivity in nanocrystalline cerium oxide exhibit a clear grain size dependence. Experimental results compiled from the literature were analyzed using a space charge model, which takes into account the deviation of point defect concentrations from their bulk values in the vicinity of grain boundaries. The consequences on conductivity arising from such space charge layers were calculated using the brick-layer model (BLM) for grain sizes L large compared to the screening length λ. The obtained results were supplemented by the calculated conductivity in the flat-band limit for $L \ll \lambda$. This combination allowed for a quantitative comparison with experimental values, which were obtained in the mesoscopic regime of grain sizes from 10–40 nm. The analysis yielded a value for the space charge potential in cerium oxide of 0.55 V. This space charge potential is caused by a reduced standard chemical potential of oxygen vacancies in the grain boundary core as compared to the bulk phase.

Keywords: cerium oxide, grain size, nanocrystalline, conductivity, space charge, brick-layer model

1. Introduction

Metal oxides of the fluorite crystal structure, such as cubic zirconia or ceria, are known to be fast oxygen ion conductors [1, 2]. Unlike zirconia, cerium oxide does not require the addition of dopants for stabilization of the cubic structure and has therefore been used as a model system for investigations of electrical conductivity at low doping concentrations. Cerium oxide is prone to deviation from the stoichiometric composition by the release of oxygen to the gas phase. This propensity to reduction gives rise to an enhanced electronic charge carrier density and renders cerium oxide a mixed ionic/electronic conductor (MIEC) [3]. In thermodynamic equilibrium, the total electrical conductivity can be related to the temperature T, oxygen partial pressure p_{O_2} in the surrounding gas atmosphere and to the concentration of low-valent cation impurities which act as acceptor ions $[A'_{Ce}]$ [1, 3, 4].

Recent studies on the electrical conductivity of nanocrystalline cerium oxide demonstrate that the grain size also has a significant effect on electrical conductivity. Under conditions in terms of T, p_{O_2} and $[A'_{Ce}]$, at which microcrystalline cerium oxide exhibits predominantly ionic conductivity, nanocrystalline cerium oxide was found to be electronic conductive [5–10]. The magnitude of electronic conductivity was higher if compared to the corresponding partial conductivity of microcrystalline or single crystalline cerium oxide and was associated with an enhanced non-stoichiometry of the nanocrystalline materials. This interpretation was supported by the observation of a much lower activation energy for the temperature dependence of electronic conductity which indicated a lower heat of reduction in this material [5, 7–9]. As noticed in all studies, the enhanced non-stoichiometry of nanocrystalline cerium oxide may be related to the large grain boundary area per unit volume in these materials and reflects the difference in reducibility (i.e. defect chemistry) at the grain boundaries as compared to the crystal lattice. It is important to notice, that such a difference in defect chemistry between grain boundary core and lattice is the origin of long range space charge potentials which are

established to equilibrate the electrochemical potentials of the various defects [11]. The defect chemistry of a polycrystalline material, in which space charge layers exist along grain boundaries, is no longer subjected to the requirement of local charge neutrality. This is particularly important, if the grain size is small and the space charge layers take up a significant volume fraction of the whole crystallite. As a consequence, the application of relationships which were derived for the volume phase under the assumption of charge neutrality may not be appropriate for a quantitative analysis of experimental results on polycrystalline materials.

Since space charge layers are not included in the point defect chemistry of the volume phase, a refined model for polycrystalline ionic solids was introduced by Maier [12]. Space charge layers along grain boundaries, characterized by their space charge potential, were incorporated into the brick-layer model to calculate the electrical conductivity for a given grain size. This space charge model was recently applied to polycrystalline cerium oxide and the calculated results were in qualitative agreement with experimental data [13]. In principle, the space charge potential, which is *a priori* unknown, could be determined by a quantitative comparison of experimental and theoretical results. However, such a comparison was not possible so far because the space charge model was limited to large grain sizes ($>$80 nm) whereas the experimental results were obtained with samples of grain sizes less than 40 nm.

In the present study, a first approach towards a quantitative comparison of experimental and theoretical results is reported. The experimental data base was extended by compiling all results reported in literature on the grain size dependence of electrical conductivity in cerium oxide. Despite of differences in sample preparation and characterization, it was possible to derive the general trend which stands out against the scattering in quantities obtained from single measurements. Furthermore, the electrical conductivity in the flat-band limit was included in the space charge model which allowed for a more reliable extrapolation of the electrical conductivity in the mesoscopic size range. The major objective of this study was to analyze the experimental data by means of the space charge model in order to derive the value of the space charge potential in polycrystalline cerium oxide.

2. Experimental Results

Various methods for synthesis and characterization of nanocrystalline cerium oxide were employed in the studies, from which experimental results were compiled for the present work. Nanocrystalline cerium oxide was prepared by decomposition of chemical precursors [5, 8, 14] or gas condensation [5, 7, 9, 10]. Except for the measurements on spin-coated films [8], nanocrystalline powders were obtained and consolidated by uniaxial pressing either at room temperature, followed by a sintering treatment [7, 9], or by hot-pressing [5, 10]. The grain size of the nanocrystalline specimens were characterized by an analysis of X-ray diffraction peak broadening [8–10], transmission-electron microscopy [5] or field emission scanning-electron microscopy [7]. Unfortunately, there is no information available in most studies on the concentration of typical acceptor ion impurities such as lanthanum or yttrium.

In all studies, the electrical conductivity was determined by an analysis of ac-impedance spectra. A common observation was, that the impedance spectra of nanocrystalline cerium oxide exhibited essentially a single semi-circle associated with the impedance of the bulk phase. Coarse grained cerium oxide, to the contrary, showed a large second arc in addition to the bulk semi-circle, due to the contribution from grain boundaries of high resistivity. Taking into account the large number of grain boundary intercepts per unit length, an analysis based on the brick-layer model suggested that the excess resistance per grain boundary was almost negligible in nanocrystalline cerium oxide.

Reported values for the electrical conductivity of nanocrystalline cerium oxide are shown as function of grain size in Fig. 1. Despite the scattering in the data, a clear trend is discernible indicating that the conductivity increases with decreasing grain size. The observation of a significant oxygen partial pressure dependence (not further discussed in the present paper) has led to the interpretation that the measured total conductivity in nanocrystalline cerium oxide is dominated by the electronic contribution. A possibility to assess the absolute values of conductivity is a comparison with the electronic conductivity of undoped single crystalline cerium oxide. This conductivity, calculated for a temperature of 500°C as 1×10^{-7} S/cm [10] characterizes the cross-over between acceptor- and donor doped cerium oxide. If the concentration

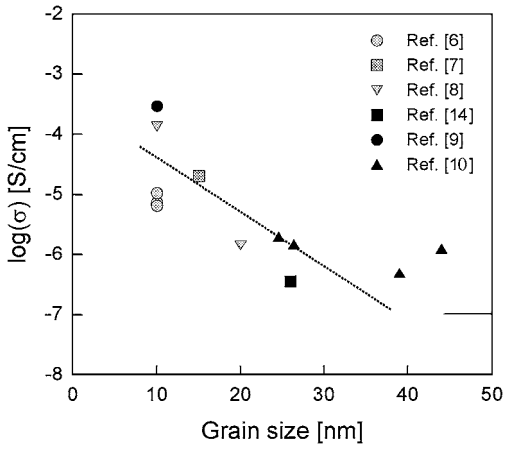

Fig. 1. Experimental results on the electrical conductivity of nanocrystalline cerium oxide as function of grain size, compiled from the given literature. Where necessary, measured conductivities were extrapolated to $T = 500°C$ and $p_{O_2} = 0.21$ atm.

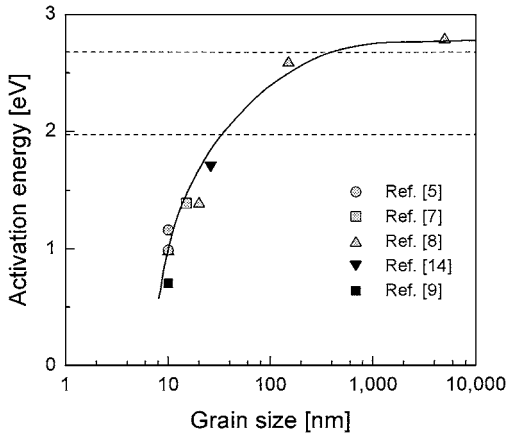

Fig. 2. Activation energy of electrical conductivity in nanocrystalline cerium oxide as function of grain size, compiled from the given literature. The lower and upper bounds for cerium oxide volume phase are marked as dashed lines.

of penta- or hexa-valent donor-type impurities can be neglected, this value represents the upper limit for the partial electronic conductivity of cerium oxide. At the smallest grain size of 10 nm, the measured conductivities were up to three orders of magnitude larger than this upper limit, Fig. 1. Since the grain boundary density also increases with decreasing grain size, the enhancement may be interpreted as a donor effect of the grain boundaries. However, it should be noticed that this increase in conductivity by more than two orders of magnitude was due to a reduction in grain size by a factor of only four, therefore indicating that this enhancement does not scale linearly with the total grain boundary area, which is inversely proportional to the grain size.

The second quantity, compiled from the various studies, is the activation energy, characterizing the temperature dependence of electrical conductivity, as a function of grain size, Fig. 2. With decreasing grain size, a steep decrease of the activation energy is observed. For the cerium oxide volume phase, the activation energy of electronic conductivity is related to the activation energy of electron hopping $E_{A,\mu}$ and the heat of reduction ΔH_R. Depending on the ratio of electron density n to the acceptor concentration $[A'_{Ce}]$, the activation energy is given as

$$E_A = E_{A,\mu} + \frac{1}{3}\Delta H_R \quad \text{for } n \gg [A'_{Ce}], \qquad (1a)$$

$$E_A = E_{A,\mu} + \frac{1}{2}\Delta H_R \quad \text{for } n \ll [A'_{Ce}]. \qquad (1b)$$

These two quantities are lower and upper bounds for the activation energy of electronic conduction in the volume phase. Based on literature data $E_{A,\mu} = 0.4$ eV [15] and $\Delta H_R = 4.67$ eV [3], these boundary values were calculated and marked in Fig. 2. Obviously, the activation energy of nanocrystalline cerium oxide decreased well below the lower limit for the volume phase. It is tempting to use Eqs. (1a) and (1b) to analyze the measured data, which would result in correspondingly small values for ΔH_R. However, the derivation of these equations is based on the assumption of local charge neutrality and they are therefore not appropriate for a quantitative analysis if space charge effects are significant. In fact, the consequences of the inhomogeneous distribution of charge carriers on the overall electrical conductivity cannot be described by such simple relationships. Instead, the space charge model for the conductivity of polycrystalline ionic materials, described by Maier [12] and adapted for application on cerium oxide [13] will be employed in the following section to analyze the experimental results.

3. Space Charge Model

The existence of space charge layers along extended structural defects in ionic solids is a consequence of thermodynamic equilibrium [16, 17]. The space charge potential is related to differences in the defect chemistry between the core of a grain/phase boundary and

the volume phase [11]. Each point defect is associated with a standard chemical potential, which is identical to the molar free energy of formation. In thermodynamic equilibrium, local defect concentrations and electrical potential are established such that the electrochemical potential of each defect is constant throughout the material. The resulting spatial variation of the electrical potential is a solution of the Poisson-Boltzmann differential equation.

$$\nabla^2\Phi(\vec{r}) = -\frac{e_0}{\epsilon\epsilon_0}\sum_i z_i \exp\left(-\frac{\mu_i^0(\vec{r}) + z_i e_0 \Phi(\vec{r})}{k_B T}\right) \tag{2}$$

Notice, that the standard chemical potentials μ_i^0 are assumed to be different in the grain boundary core and the bulk lattice. For given values of μ_i^0, Eq. (2) can be solved to derive the electrical potential $\Phi(\vec{r})$. The result of a numerical solution for a planar grain boundary is shown in Fig. 3. It can be shown that for pure cerium oxide, a significant positive space charge potential can only be due to a reduced standard chemical potential of oxygen vacancies $\mu^0_{V_{\ddot{O}}}$ in the grain boundary core as compared to the bulk value. Furthermore, the magnitude of the space charge potential is essentially determined by the difference $\Delta\mu^0_{V_{\ddot{O}}} = \mu^0_{V_{\ddot{O},gb}} - \mu^0_{V_{\ddot{O},bulk}}$ but almost independent of the absolute values of μ_i^0. As shown in the example of Fig. 3, a difference of $\Delta\mu^0_{V_{\ddot{O}}} = -1.8$ eV result is a space charge potential

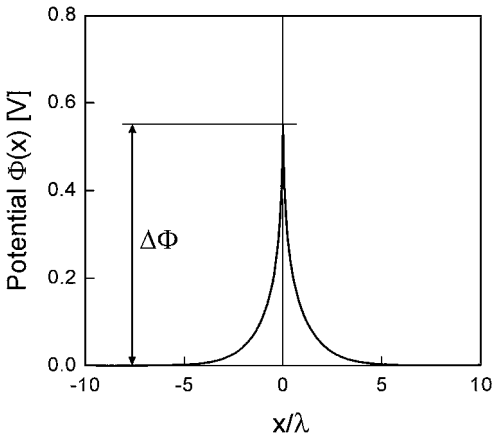

Fig. 3. Variation of the electrical potential across a grain boundary, obtained by numerical solution of Eq. (2) assuming a width for the grain boundary core of 1 nm and $\mu^0_{V_{\ddot{O},gb}} - \mu^0_{V_{\ddot{O},bulk}} = -1.8$ eV.

$\Delta\Phi = 0.55$ V [18]. This space charge potential can be regarded as a new material parameter, characteristic of the grain boundary defect chemistry. The magnitude of this quantity, which is generally unknown, may be obtained by comparing experimental results and theoretical predictions with $\Delta\Phi$ as an adjustable parameter. In the following, the electrical conductivity of polycrystalline cerium oxide will be calculated as function of grain size and compared with the experimental results presented above.

The most important implication of the space charge potential is the corresponding concentration profile of point defects perpendicular to the interface. Under some simplifying assumptions, an analytic expression for the defect concentration at distance x from the grain boundary can be derived [19],

$$\frac{c_i(x)}{c_{i0}} = \left(\frac{1 + \Theta\ \exp(-x/\lambda)}{1 - \Theta\ \exp(-x/\lambda)}\right)^{2z_i}, \tag{3}$$

with c_{i0} being the bulk concentrations of the defect species and two characteristic parameters, the screening length

$$\lambda = \left(\frac{\epsilon\epsilon_0 k_B T}{\sum_i (z_i e_0)^2 c_{i0}}\right)^{1/2} \tag{4}$$

and a profile parameter

$$\Theta = \tanh\left(\frac{z e_0 \Delta\Phi}{4 k_B T}\right). \tag{5}$$

In thermodynamic equilibrium, the bulk defect concentrations and the screening length λ are completely determined by T, p_{O_2} and $[A'_{Ce}]$, whereas Θ is depending on the space charge potential and temperature. The calculated concentration profiles of electrons, oxygen vacancies and acceptor ions are shown in Fig. 4. The effect of the space charge potential on the distribution of point defects depends on the sign of the defect charge. Given a value of $\Delta\Phi = 0.55$ V, negatively charged defects, i.e. electrons and acceptor ions, will be accumulated and positively charged oxygen vacancies will be depleted in the space charge layer. Two important consequences arise from this space charge segregation of point defects. First, the redistribution of acceptor ions, leading on the one hand to an accumulation in the space charge layer, results on the other hand in a corresponding depletion of the volume phase since the total acceptor concentration is constant [20] and can

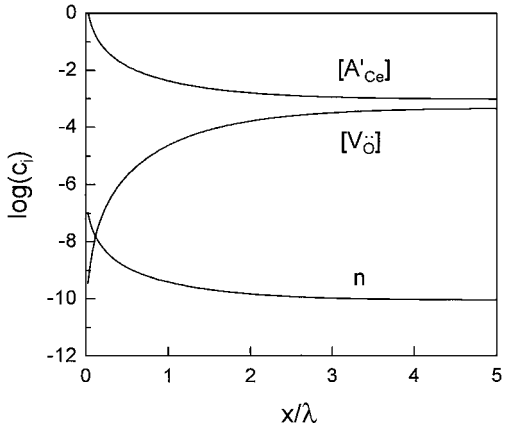

Fig. 4. Local concentration of the various point defects as function of the normalized distance from the grain boundary, calculated for a space charge potential of $\Delta\Phi = 0.55$ V and a total acceptor concentration of 1000 ppm.

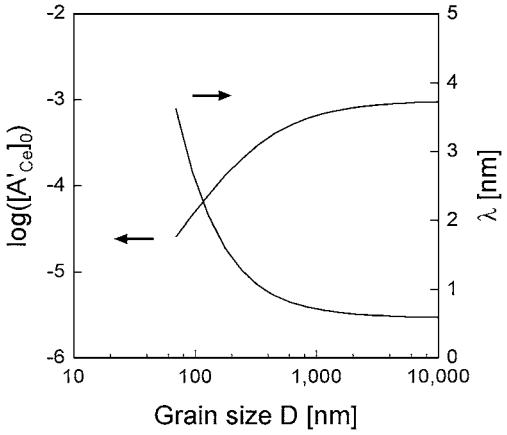

Fig. 5. Residual bulk concentration of acceptor ions and screening length λ as function of grain size for a space charge potential $\Delta\Phi = 0.55$ V and a total acceptor concentration of 1000 ppm.

be expressed for a polycrystalline material with grain size D in terms of their bulk concentration, the screening length λ and the profile parameter θ [13]. This relationship can be used to calculate the residual bulk concentration $[A'_{Ce}]_0$ for a given total acceptor concentration $[A'_{Ce}]_{tot}$,

$$[A'_{Ce}]_0 = [A'_{Ce}]_{tot}\left((1-\psi_{sc}) + \psi_{sc}\frac{1-\Theta}{1+\Theta}\right)^{-1}. \quad (6)$$

The quantity ψ_{sc} depicts the effective volume fraction of space charge layers of thickness $k\lambda$ in the polycrystalline material of grain size D,

$$\psi_{sc} = 6\frac{k\lambda}{D}. \quad (7)$$

The prefactor k depends on the charge of the majority defect which is accumulated in the space charge layer under the given conditions with $k = 2$ for $|z| = 1$ and $k = \frac{8}{3}$ for $|z| = 2$ [13]. It should be noticed that the screening length also depends on the bulk concentration of the acceptor ions. Therefore, Eq. (6) is only implicit and $[A'_{Ce}]_0$ has to be calculated by iteration. The effect of acceptor segregation on the residual bulk concentration and the screening length is shown in Fig. 5. The redistribution of acceptor ions has two important consequences.

First, the decrease in the bulk concentration of acceptor ions directly affects the bulk concentrations of the mobile charge carriers in such a way that the ionic

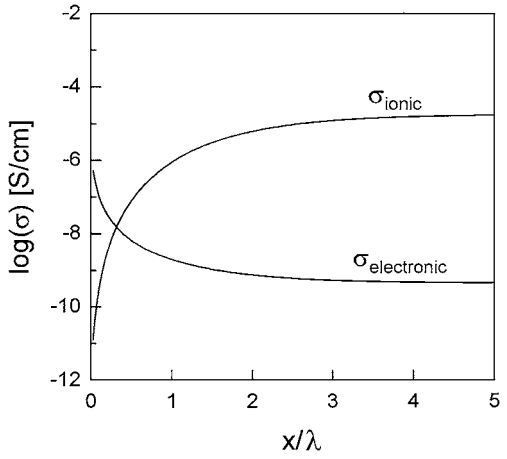

Fig. 6. Local ionic and electronic partial conductivities as function of the normalized distance from the grain boundary, calculated for a space charge potential of $\Delta\Phi = 0.55$ V and a total acceptor concentration of 1000 ppm.

bulk conductivity decreases and the electronic bulk conductivity increases. The second consequence is the variation of local ionic and electronic conductivity in the vicinity of grain boundaries, Fig. 6 [12]. Depending on the magnitude of the space charge potential, this effect may even lead to an inversion layer as indicated in Fig. 6. Obviously, the accumulation of electrons and depletion of oxygen vacancies in the space charge layer will result in an enhanced electronic and reduced ionic conductivity in the boundary layer. In order to quantify this effect, it is necessary to incorporate the calculated

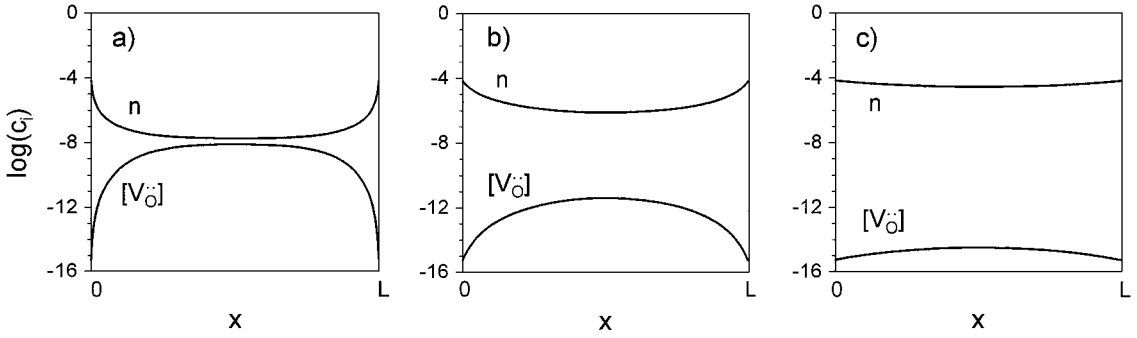

Fig. 7. Concentration profiles for oxygen vacancies and electrons across an infinite plate of cerium oxide with thickness (a) $L = 10\,\lambda$, (b) $L = \lambda$, and (c) $L = 0.1\,\lambda$, obtained by numerical solution of Eq. (2).

concentration profiles into a structural model representative of a polycrystalline material.

As long as the grain size is large compared to the screening length λ, the brick-layer model (BLM) can be employed for this purpose [12]. If the grains are at least one order of magnitude larger than the screening length, the center part of the crystal is essentially charge neutral and the defect concentrations are determined by the volume defect chemistry. The concentration profiles in the boundary layers can be approximated by the solution for planar interfaces given above, Fig. 7(a). The total electrical conductivity is calculated according to the equivalent cirquit for the BLM. Details on the mathematical treatment can be found in [12, 13]. With regards to the constraint $L \gg \lambda$ and the grain size dependence of λ, shown in Fig. 5, the brick-layer model described above can be applied to calculate the electrical conductivity for grain sizes above 80 nm.

If the grain size and screening length are on the same order of magnitude, the space charge layers from opposite grain boundaries overlap and the solution given in Eq. (3) is not applicable, Fig. 7(b). Analytical solutions can still be found for two parallel plates at distance $L \approx \lambda$ and applied to describe the space charge potential in thin films [21]. However, no solutions are available for the three-dimensional problem of a cubic crystal. Furthermore, the contribution to conductivity stemming from volume elements in the vicinity of edges and corners with their specific geometry may no longer be negligible. In this mesoscopic size range, the equations describing the defect chemistry and transport properties must be solved numerically, which is not further elucidated in the present study.

If the grain size finally becomes small as compared to λ, the whole crystal volume is occupied by space charge and the defect concentrations become constant throughout the cross section of the crystallite, Fig. 7(c). This flat band situation defines the upper limit to which the electrical conductivity will increase upon reduction of grain size. The electronic conductivity in the flat band limit is given as,

$$\sigma_{\mathrm{el,fb}} = \sigma_{\mathrm{el},0}\ \exp\left(\frac{e_0 \Delta\Phi}{k_B T}\right), \tag{8}$$

with $\sigma_{\mathrm{el},0}$ being the bulk conductivity at the same temperature, oxygen partial pressure and $[A'_{Ce}] = 0$.

In summary, two analytic expressions for the conductivity of polycrystalline cerium oxide were derived. Depending on the relative magnitude of grain size and screening length, the electrical conductivity could calculated either using the space charge model based on Eq. (3) for $L \gg \lambda$ or using the flat-band result for $L \ll \lambda$.

The grain sizes of the measured samples, ranging from 10–40 nm, lie in between the size ranges in which either the brick-layer model or the flat band limit is valid. As mentioned above, the electrical conductivity in this mesoscopic regime might be modeled by numerical calculations, as will be shown in a following paper. An alternative approach is to extrapolate the results derived from the space charge model for $L \gg \lambda$ to small grain sizes. It is safe to assume that the conductivity will change continuously and monotonically with grain size and will approach to the flat-band value at grain sizes $L \ll \lambda$. Following this strategy, the grain size dependence of electrical conductivity was calculated using different values for the space charge potential and compared with experimental results.

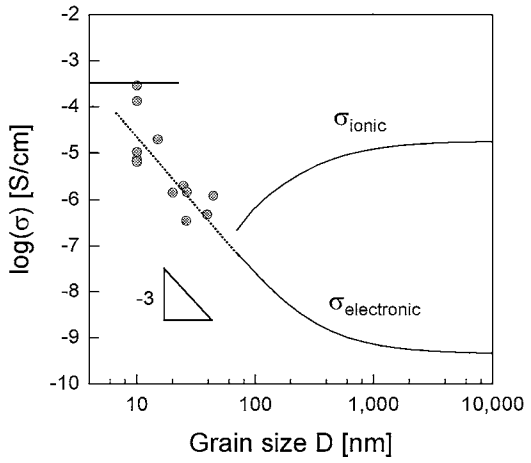

Fig. 8. Electrical conductivity of polycrystalline cerium oxide as function of grain size. The result of the space charge model (solid lines) for σ_{el} is extrapolated (dotted line) based on the flat band limit. The best agreement with the experimental results, as presented in Fig. 1, was obtained for $\Delta\Phi = 0.55$ V.

4. Results and Discussion

The following calculations were performed for $T = 500^{\circ}$C, $p_{O_2} = 0.21$ atm and $[A'_{Ce}] = 1000$ ppm. The former two values are given by experimental conditions whereas the latter value was assumed to be a typical impurity concentration (the scattering in the experimental results may originate to some degree from deviations of this quantity in the individual samples). In Fig. 8, theoretical and experimental results on the electrical conductivity of polycrystalline cerium oxide as function of grain size are compared. As discussed above, calculations based on the brick-layer model were limited to grain sizes larger than 80 nm. Under the given conditions, the electrical conductivity of cerium oxide with large grain size is dominated by the ionic contribution. As a consequence of defect accumulation/depletion in space charge layers, the ionic partial conductivity decreases with decreasing grain size whereas the electronic conductivity incrases, resulting in a transition from predominantly ionic to electronic conductivity at a grain size of about 60 nm. The extrapolated increase of electronic conductivity beyond the size range of the BLM-calculation is justified by the flat-band value, to which the electronic conductivity should approach at small grain sizes. Based on this extrapolation, the best agreement between calculated and experimental results was achieved for a space charge potential of $\Delta\Phi = 0.55$ V. The space charge model correctly predicts absolute values of electronic conductivity larger than the acceptor/donor cross-over values of 1×10^{-7} S/cm. Electronic conductivity above this value could be achieved in the volume phase of cerium oxide only by doping with penta- or hexavalent donor ions. Furthermore, a rather steep increase of conductivity with decreasing grain size, characterized by a slope of ≈ -3 in Fig. 8, is consistent with the experimental results and indicates that the grain size effect does not scale linearly with the grain boundary area per unit volume.

The second experimental result, which exhibited a large grain size effect was the activation energy, Fig. 2. The space charge model was used to calculate the electrical conductivity of polycrystalline cerium oxide at different temperatures. An Arrhenius analysis of the calculated conductivities provided the activation energies of the partial conductivities as function of grain size. The results are shown in Fig. 9 for an oxygen partial pressure of $p_{O_2} = 10^{-20}$ atm. The choice of this very low oxygen partial pressure involves two aspects which will be elucidated in the following.

Given a space charge potential of $\Delta\Phi = 0.55$ V, the activation energy in the flat band limit,

$$E_{A,el,fb} = E_{A,\mu} + \frac{1}{3}\Delta H_R - e_0\Delta\Phi, \qquad (9)$$

can be calculated as 1.41 eV. In analogy to the flat band value of electronic conductivity, the activation

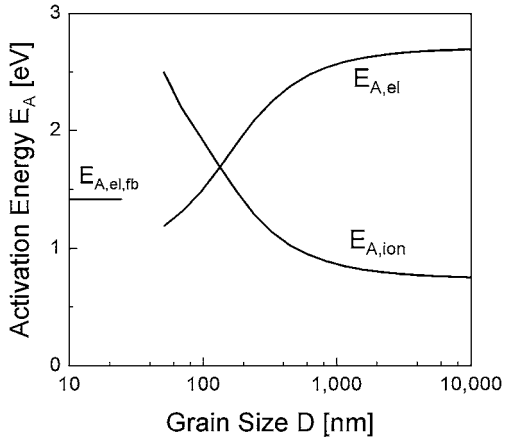

Fig. 9. Activation energy of ionic and electronic partial conductivity as function of grain size for $p_{O_2} = 10^{-20}$ atm. Notice the decrease of $E_{A,el}$ below the flat band limit and the increases of $E_{A,ion}$ at small grain sizes.

energy should approach to this value as the grain size becomes much smaller than the screening length λ. This would agree with the experimental observation of activation energies below the lower limit of 1.98 eV for the volume phase. However, some experimental results were even lower than the flat band value of 1.41 eV. This apparent inconsistency is due to the fact, that the flat band limit for the activation energy is not a lower bound. As evident from Eq. (9), the flat band value of 1.41 eV is independent of the oxygen partial pressure. Therefore, we may calculated the grain size dependent activation energy for any value of p_{O_2} and compare these activation energies with the flat band limit without loss of generality.

The second aspect is related to the limitation of the space charge model to grain sizes $L \gg \lambda$. By chosing a low oxygen partial pressure, it was possible to demonstrate the steep decrease of the activation energy within the valid range of grain sizes for the brick-layer model. As shown in Fig. 9, the activation energy $E_{A,el}$ at $p_{O_2} = 10^{-20}$ atm and grain sizes below 100 nm became smaller than the flat band value. The additional reduction of $E_{A,el}$ is caused by the temperature dependence of acceptor segregation and this contribution is most significant in the mesoscopic regime.

This consideration shows, that the flat-band value for the activation energy is not a lower bound and the extrapolation of activation energies into the size range between the BLM and the flat band limit and thus a direct comparison of theoretical and experimental results is not reasonable as long as numerical calculations in the mesoscopic regime are not available. Nevertheless, the qualitative result of a steep decrease in activation energy $E_{A,el}$ with smaller grain size is in qualitative agreement with experimental results. It is also interesting to notice, that the space charge model predicts an increasing activation energy for the ionic partial conductivity, which may explain the unusually high value of 1.6 eV reported in [22].

As mentioned above, the activation energy of the cerium oxide volume phase $E_{A,el}$ may be analyzed according to Eq. (1a) and (1b). If the activation energy of electron mobility is not significantly affected by the grain size [22], the application of this analysis to the experimental results from nanocrystalline cerium oxide would imply a grain size dependent enthalpy of the oxygen exchange equilibrium ΔH_R [8]. However, this effective enthalpy is not an average of bulk and grain boundary contributions following a simple rule of mixing. It is reasonable to assume that the grain boundary core in polycrystalline cerium oxide is more reduced than the bulk phase, based on the enhanced reduction of the cerium oxide surface [23, 24]. As shown in Fig. 3, a space charge potential of 0.55 V is established if the standard chemical potential for oxygen vacancies in the grain boundary core is reduced by 1.8 eV as compared to the bulk value. If the electronic structure in the grain boundary core is not too different from the bulk phase, this decrease translates into a correspondingly lower value for $\Delta H_{R,gb} = 4.67\ \text{eV} - 1.8\ \text{eV} \approx 2.9\ \text{eV}$ in the grain boundary core. The enhanced propensity to reduction at the grain boundary core, characterized by this value of $\Delta H_{R,gb}$, and the consequences on the distribution of point defects, as described by the space charge model, are consistent with the experimental results.

5. Summary

The grain size of nanocrystalline cerium oxide has a significant impact on the magnitude and activation energy of electrical conductivity. Both effects were consistently described by a model, which takes into account space charge layers along grain boundaries. As a consequence of space charge segregation of point defects, the ionic partial conductivity in cerium oxide decreases and the electronic conductivity increases with decreasing grain size for positive space charge potentials. The best quantitative agreement between experimental and theoretical results was obtained for a space charge potential of 0.55 V. The analysis of equilibrium between grain boundary core and bulk phase revealed, that this space charge potential was caused by the standard chemical potential of oxygen vacancies, which is reduced by ca. 1.8 eV in the core of grain boundaries as compared to the bulk.

Acknowledgment

The authors would like to acknowledge financial support by the Deutsche Forschungsgemeinschaft (SFB 277, "Grenzflächenbestimmte Materialien") and the Fonds der Chemischen Industrie.

References

1. H.L. Tuller and A.S. Nowick, *J. Electrochem. Soc.*, **122**, 255 (1975).
2. B.C.H. Steele, *Solid State Ionics*, **129**, 95 (2000).

3. H.L. Tuller and A.S. Nowick, *J. Electrochem. Soc.*, **126**, 209 (1979).
4. H.L. Tuller, in *Nonstoichiometric Oxides*, edited by T.O. Sørensen (Academic Press, New York, 1981), p. 271.
5. Y.-M. Chiang, E.B. Lavik, I. Kosacki, H.L. Tuller, and J.Y. Ying, *Appl. Phys. Lett.*, **69**, 185 (1996).
6. Y.-M. Chiang, E.B. Lavik, I. Kosacki, H.L. Tuller, and J.Y. Ying, *J. Electroceramics*, **1**, 7 (1997).
7. J.H. Hwang and T.O. Mason, *Z. Phys. Chem.*, **207**, 21 (1998).
8. I. Kosacki, T. Suzuki, and H.U. Anderson, in *Solid State Ionic Devices*, ECS Proceedings Vol. 99-13, edited by E.D. Wachsman, M.-L. Liu, J.R. Akridge, and N. Yamazoe (Electrochemical Society, Pennington, 1999), p. 190.
9. A. Tschöpe, J.Y. Ying, and H.L. Tuller, *Sensors & Actuators*, **B31**, 111 (1992).
10. A. Tschöpe, E. Sommer, and R. Birringer, *Solid State Ionics*, **139**, 255 (2001).
11. J. Jamnik, J. Maier, and S. Pejovnik, *Solid State Ionics*, **75**, 51 (1995).
12. J. Maier and Ber. Bunsenges, *Phys. Chem.*, **90**, 26 (1986).
13. A. Tschöpe, *Solid State Ionics*, **139**, 267 (2001).
14. E. Sommer, Impedanzspektroskopie an nanokristallinem Ceroxid. Diploma thesis, Universität des Saarlandes, 1997.
15. H.L. Tuller and A.S. Nowick, *J. Phys. Chem. Solids*, **38**, 859 (1977).
16. J. Frenkel, *Kinetic Theory of Liquids* (Oxford University Press, New York, 1946).
17. K.L. Kliewer and J.S. Koehler, *Phys. Rev.*, **140**, 1226 (1965).
18. A. Tschöpe, to be published.
19. D.F. Evans and H. Wennerström, *The Colloidal Domain* (VCH Publisher, New York, 1994).
20. M. Aoki, Y.-M. Chiang, I. Kosacki, L.J.-R. Lee, H.L. Tuller, and Y. Liu, *J. Am. Ceram. Soc.*, **79**, 1169 (1996).
21. J. Maier, *Solid State Ionics*, **23**, 59 (1987).
22. J.-H. Hwang, D.S. McLachlan, and T.O. Mason, *J. Electroceramics*, **3**, 7 (1999).
23. H.C. Yao and Y.F. Yu Yao, *J. Catal.*, **86**, 254 (1984).
24. D.C. Sayle, S.C. Parker, and C.R.A. Catlow, *Surf. Sci.*, **316**, 329 (1994).